Applied Catalysis B: Environmental 294 (2021) 120238

Contents lists available at ScienceDirect

Applied Catalysis B: Environmental

journal homepage: www.elsevier.com/locate/apcatb

Covalent organic framework-supported Zn single atom catalyst for highly efficient N-formylation of amines with CO_2 under mild conditions

Qiang Cao [a], Long-Long Zhang [a], Chang Zhou [a], Jing-Hui He [a,*], Antonio Marcomini [b], Jian-Mei Lu [a,*]

[a] College of Chemistry, Chemical Engineering and Materials Science, Collaborative Innovation Center of Suzhou Nano Science and Technology, National United Engineering Laboratory of Functionalized Environmental Adsorption Materials, Soochow University, Suzhou, 215123, PR China
[b] Department of Environmental Sciences, Informatics and Statistics, University Ca' Foscari Venice, Via Torino 155, Venezia Mestre, 30170, Italy

ARTICLE INFO

Keywords:
Single atom catalyst
Carbon dioxide
Mild conditions
TOF
Reusability

ABSTRACT

Transformation of CO_2 into value-added chemicals with efficient and recyclable catalyst is an effective way to reduce carbon emissions. It is valuable to develop an efficient catalyst that can promote the N-formylation reaction under mild conditions with a high activity and excellent recyclability. Single atom catalysts (SACs) possess ultimate atom utilization efficiency and outstanding catalytic performance. Herein, we synthesize Zn SACs (Zn-TpPa) anchored on a COF (TpPa-1) using a facile solution method. Catalyzed by Zn-TpPa, CO_2 and N-methylamine are transformed into N-methylformanilide under mild reaction conditions with a TOF of 17,155 h^{-1}, which is the highest among all reported recyclable Zn-based catalysts. Zn-TpPa can also catalyze N-formylation of many other amines with excellent yields. The higher reactivity was attributable to the well-dispersed Zn active sites on COF and outstanding adsorption of CO_2 owing to high surface area of COF. Our research provides a facile method for constructing SACs as well as an effective pathway for CO_2 transformation and environmental protection.

1. Introduction

Carbon dioxide (CO_2), known as the main factor for green-house effect, has stimulated much effort to develop efficient technologies and methods for decreasing the CO_2 level in the atmosphere. [1–5] As CO_2 is a non-toxic, abundant, renewable C1 building block, easily available and environmentally benign feedstock, in view of green and sustainable chemistry, designing recyclable catalysts for the transformation of CO_2 into value-added chemicals has recently emerged as an attractive route. [6–23] One interesting route to fix CO_2 is synthesis of formamides through N-formylation of amines using CO_2 in the presence of reducing agent. Many catalysts were reported to promote this reaction. [10,16,24–30] However, those reported N-formylation catalysis either have a limited turnover frequency (TOF) [21,31–36] or require harsh conditions, such as high reaction temperatures (>60 °C) [7,15,21,25,34,36–38] or high CO_2 pressure (>1 Mpa) [6,7,13–15,21,32,33,37–40] and poor recyclability [35]. It is highly desirable to develop an efficient catalyst that can promote the N-formylation reaction under mild conditions with a high TOF and excellent recyclability.

Single-atom catalysts (SACs), containing single metal atoms anchored on solid supports, represent the utmost utilization of metallic catalysts and thus maximize catalytic reactivity. [41–45] Several fabrication processes for SACs have been reported [46], including atomic layer deposition, [47] wet chemistry [48], MOF derivative [49], potential cycling [50], acid leaching [51] and photodeposition [52]. However, they usually either require harsh conditions, such as high temperature, high pressure, acids or complicated reaction procedures. Considering the large-scale production in future industrialization, a simple and efficient way to achieve SACs is more favorable. An appropriate support is critical to interact strongly with isolated atoms, and thus prevents the movement and aggregation of isolated atoms [53–55], creating stable, finely dispersed active sites.

Covalent organic frameworks (COFs) represent an important type of covalent porous materials with high surface area and well-defined structures. [56,57] The periodic and permanent porosity endow COFs an excellent substrate for SACs [58]. The bottom-up synthesis using different building blocks endows COFs with tunable skeleton structure, pore size, and topology schemes [53,59,60]. With the bottom-up

* Corresponding authors.
E-mail addresses: jinghhe@suda.edu.cn (J.-H. He), lujm@suda.edu.cn (J.-M. Lu).

https://doi.org/10.1016/j.apcatb.2021.120238
Received 18 February 2021; Received in revised form 8 April 2021; Accepted 15 April 2021
Available online 20 April 2021

synthesis of COFs followed by post-metalation, it offers unprecedented opportunities for constructing SACs with well-defined catalytic centers in high metal loading [61].

Herein, we demostrate Zn single atom catalyts can be prepared on COF (TpPa-1) with high loading amount by facile dropwise adding Zn^{2+} solution into TpPa-1 suspension (Scheme 1) [62,63]. Catalyzed by Zn-TpPa, N-methylformanilide is produced by reacting N-methylaniline with CO_2 and hydrosilanes under mild reaction conditions (1 bar CO_2 pressure at room temperature) in 3 h with a TOF of 17,155 h^{-1}, which is the highest among reported recyclable Zn-based catalysts. Besides, Zn-TpPa could catalyze N-formylation of many other amines with excellent yields. Our research provides a simple yet efficient method for constructing SACs as well as provides an effective and sustainable pathway for CO_2 transformation and environmental protection.

2. Experimental section

2.1. Materials and characterizations

1,3,5-triformylphloroglucinol (Tp) and p-phenylenediamine (Pa-1) were purchased from Shanghai Macklin Biochemical Co. Ltd. N-methylaniline, aniline, p-toluidine, N-methyl-p-toluidine, 4-methoxy-N-methylaniline, 4-bromo-N-methylaniline, N-methylcyclohexylamine, diethylamine, pyrrolidine, morpholine, 1,2,3,4-Tetrahydro-1-methylquinoline, and phenylsilane were obtained from J&K Scientific Ltd. N, N-dimethylformamide, acetonitrile mesitylene, dioxane and methanol were obtained from Aladdin Industrial Corporation (Shanghai, China).

Scanning electron microscopy (SEM) images were recorded by HITACHI S4700. Transmission electron microscopy (TEM) images were captured by Tecnai G20. Aberration-corrected high-angle annular dark-field STEM (AC-HAADF-STEM) images were acquired by FEI Titan Themis 60−300. Fourier transform infrared spectroscopy (FT-IR) spectra were acquired on BRUKER VERTEX 70. N_2 and CO_2 adsorption isotherm were acquired on ASAP2020. XRD patterns were obtained using a Multiple Crystals X-ray Diffractometer (D8 Advance). Solid-state NMR (SSNMR) spectra were measured on a Bruker Advance III HD 400 spectrometer. Inductively coupled plasma optical emission spectrometry (ICP-OES) was performed on VARIAN 710.

2.2. Synthesis of single atom catalysts M-TpPa

TpPa-1 COF was synthesized according to the procedures in literature with a little modification. [63] A pyrex tube is charged with triformylphloroglucinol (Tp) (63 mg, 0.3 mmol), p-phenylenediamine (Pa-1) (48 mg, 0.45 mmol), 1.5 mL of mesitylene, 1.5 mL of dioxane and 0.25 mL of 6 M aqueous acetic acid. The mixture was sonicated for 10 min. The tube was then flash frozen at 77 K and degassed by three freeze-pump-thaw cycles. The tube was sealed off and then heated at 120 °C for 3 days. The product was filtration and washed with anhydrous tetrahydrofuran, acetone and hexane [64]. The powder collected was then solvent exchanged with anhydrous tetrahydrofuran, acetone and hexane [64] and then dried at 120 °C under vacuum for 24 h to give TpPa-1 COF.

TpPa-1 COF (50 mg) was dispersed in 50 mL deionized water to give TpPa-1 suspension for further use. $ZnCl_2$ (73 mg, equal mole number to Nitrogen element in TpPa-1 solution) was dissolved in 50 mL deionized water. In a typical synthesis of Zn-TpPa, $ZnCl_2$ solution were added into the flask containing TpPa-1 suspension through a two-channel syringe pump at a rate of 1 mL h^{-1} under magnetic stirring at room temperature. Then the product was filtration and washed with anhydrous tetrahydrofuran, acetone and hexane [64] and then dried at 120 °C under vacuum for 12 h to give Zn-TpPa (Scheme 1) [62]. Using ultralow surface tension solvents such as hexane enable facile COF activation with reduced pore collapse [64]. Other M-TpPa COFs (M = Pt, Pd, Ni) were prepared in the same method.

2.3. Synthesis of formamide derivatives

Take the N-formylation of N-methylaniline as a template for the typical synthetic procedure of amines. $PhSiH_3$ (216.4 mg, 2 mmol), Zn-TpPa (20 mg, Zn 1.5 μmol) and DMF (1 mL) were added into 10 mL two-neck round-bottom flask that was connected to a CO_2 balloon with stirring and subjected to three vacuum and CO_2-purge cycles. Subsequently, N-methylaniline (107.2 mg, 1 mmol) was dissolved in DMF (1 mL) and added into the reactor successively using syringe injection under CO_2 and then subjected to three vacuum and CO_2-purge cycles. The reaction mixture was kept stirring at 30 °C for 12 h. Finally, the conversion and selectivity of the product were checked by GC–MS.

3. Results and discussion

3.1. Characterization of materials

We synthesized single atom catalysts Zn-TpPa by adding the aqueous Zn salt solution into TpPa-1 suspension (Scheme 1), which was synthesized according to the method as previously reported. [62,63] The composition of TpPa-1 and Zn-TpPa was assessed with X-ray photoelectron spectroscopy. The peaks at 1020 eV and 1045 eV in Zn 2p XPS

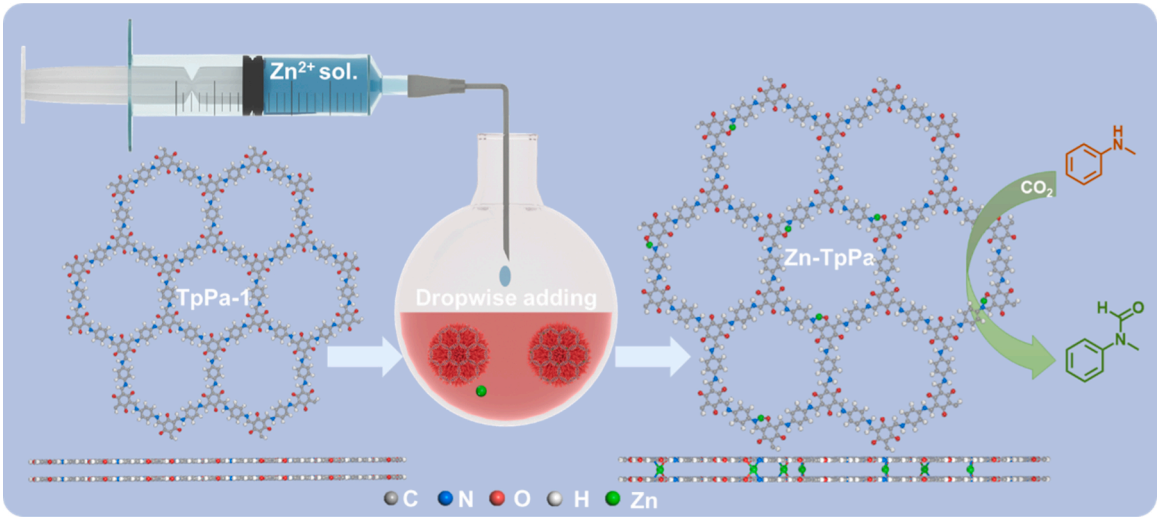

Scheme 1. Synthetic scheme of Zn-TpPa and N-formation of N-methylaniline with CO_2.

(Fig. S1d) spectrum indicated the presence of Zn element in Zn-TpPa. Besides, the Zn loading in the Zn-TpPa reached 0.5 wt%, as determined by inductively coupled plasma optical emission spectrometry (ICP-OES).

In the high-resolution XPS spectrum of O 1s of the TpPa-1 (Fig. 1c), the two binding energy peaks at 530.8 and 532.5 eV are assigned to C═O in keto-form and the end aldehyde groups in the TpPa-1 framework, respectively. [63,65] After treatment with Zn^{2+}, a new Zn-O peak (534.3 eV) formed, and the peak located at 530.8 eV of the TpPa-1 decreased a certain level, revealing that a part of the O atoms of the C═O were coordinated to Zn^{2+}. The N 1s peak of TpPa-1 shifted from 400.2 eV to 400.1 eV in Zn-TpPa (Fig. S1c), indicating the successful coordination between Zn and N atom. From FT-IR spectra (Fig. 1b), both TpPa-1 and Zn-TpPa showed a strong peak at 1578 cm^{-1} arising from the C═C stretching and a shoulder peak at 1616 cm^{-1} corresponded to C═O stretching bands, indicating they were in the keto-form. However, the C—N peak of TpPa-1 at 1257 cm^{-1} moved to 1255 cm^{-1} in Zn-TpPa, which further revealing the interaction between Zn^{2+} and N.

To gain insight into the binding between Zn^{2+} and N, Zn (10)-TpPa (the initial reaction moles ratio of Zn/N is 10:1 to increase the Zn loading amount) and was synthesized and characterized by solid-state high-resolution ^{1}H NMR. In Fig. 1d, the pristine TpPa-1 has three different hydrogen environments as a (N-H), b (C = C–H) and c (phenyl-H) with the ratio of 1:1:2. However, in Zn(10)-TpPa, the ratio decreased to 0.75:1:2 (Fig. 1e), which indicated that Zn^{2+} replaced a part of hydrogen atoms in environment a (N-H). The overall results above infer that Zn^{2+} were chelated simultaneously by O and N atoms. DFTB calculations were used to probe the nature of the interaction of Zn^{2+} with the COF backbone. [66] They suggest the possibility of the prominent interlayer interactions of Zn^{2+} ions with nucleophilic centers of COF (Scheme 1 and Fig. S6). The C = O…Zn (2.20 Å) and N…Zn distances (2.15 Å) agree with the possibility of intermolecular interactions. [67] The AA-stacking COF/Zn^{2+} interaction further support the chelation of Zn^{2+} with O and N atoms.

Zn-TpPa (Fig. 2a and b) showed micro-flower-like morphology as revealed by SEM and TEM images, indicated the Zn loading does not alter the TpPa-1 morphology (Fig. S3a–S3d). The corresponding element mapping images (Fig. 2c) revealed a homogeneous distribution of C, N, O and Zn in Zn-TpPa. More importantly, aberration-corrected high-angle annular dark-field STEM (AC-HAADF-STEM) images showed that numerous separated Zn atoms, appearing as individual bright spots with an average size of ca. 0.2 nm were uniformly distributed over all of the TpPa-1 COF (Figs. 2d and S4). No larger particles or crystalline Zn phases were observed, validating that the identified Zn atoms were present as single atoms. [68] In addition, PXRD pattern of Zn-TpPa (Fig. 1a) shows no peak of metallic Zn. [69] XPS spectra (Fig. S1d) also show that all Zn atoms have an oxidation of +2 and therefore there should be no Zn cluster. [70] These results indicate that Zn species present as isolated single atoms.

The sharp and intense peaks at 4.7° and 26.7° corresponded to (100) and (001) planes of TpPa-1 COF. Moreover, the experimental PXRD pattern matched well with the simulated PXRD pattern, and this is no any characteristic peaks from zinc salts and metallic Zinc. The sharp peak of Zn-TpPa at 4.7° corresponding to (100) reflection plane and the similar PXRD patterns with TpPa-1 in Fig. 1a indicated that Zn-TpPa preserved the crystallinity of TpPa-1 COF with little reduction after coordinating with Zinc cation. ^{13}C NMR spectra (Fig. S1a) showed no difference between TpPa-1 and Zn-TpPa, which further supported this point.

The permanent porosities of TpPa-1 and Zn-TpPa were evaluated by measuring N_2 adsorption isotherms at 77 K. Activated TpPa-1 and Zn-TpPa both showed reversible type-I adsorption isotherms (Fig. S1b). The Brunauer-Emmett-Teller (BET) surface areas of the activated Zn-TpPa was found to be 675.9 m^2/g, nearly unchanged compared to TpPa-1 (878.7 m^2/g). Using ultralow surface tension solvents such as hexane enable facile COF activation with reduced pore collapse. [64] The slightly reduced crystallinity and BET surfaces areas were resulted from the chelation of Zn^{2+} with N and O atoms in Zn-TpPa blocked

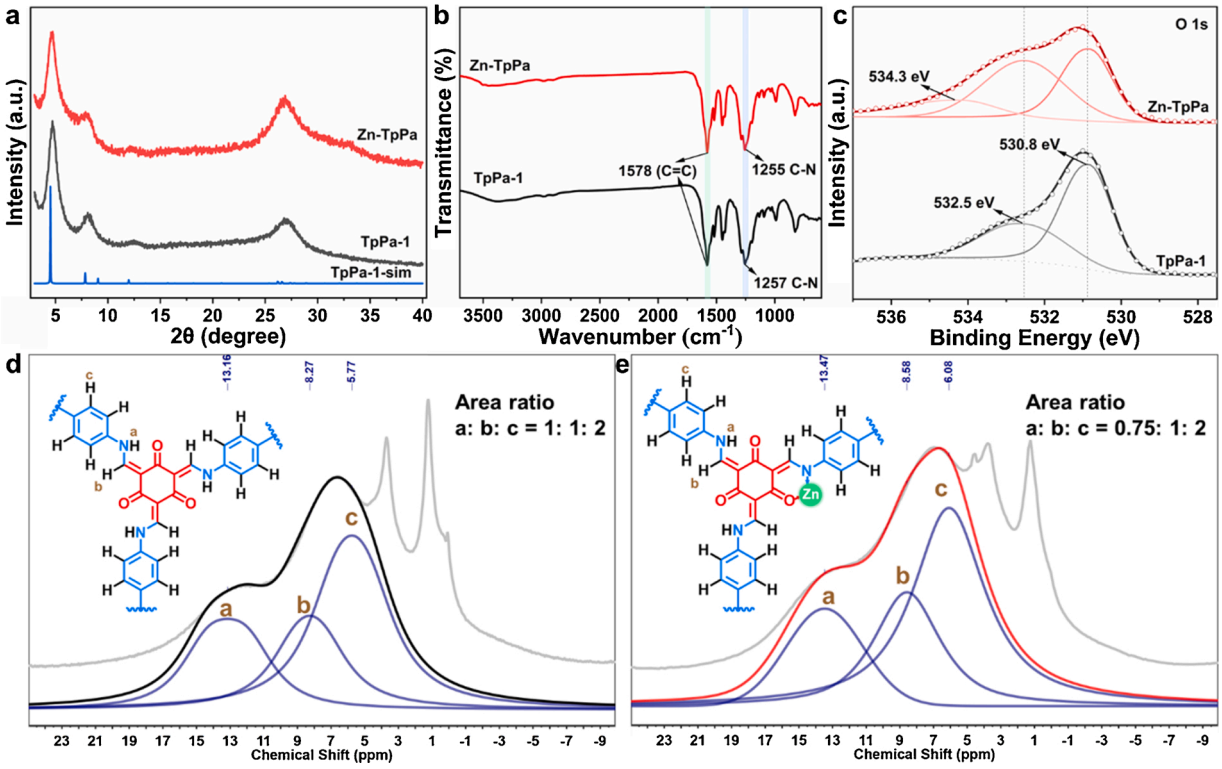

Fig. 1. Materials characterization. PXRD patterns (**a**), FT-IR spectra (**b**), O 1s XPS spectra (**c**) of pristine TpPa-1 and Zn-TpPa. ^{1}H NMR spectra with simulated peaks of pristine TpPa-1 (**d**) and Zn (10)-TpPa (**e**).

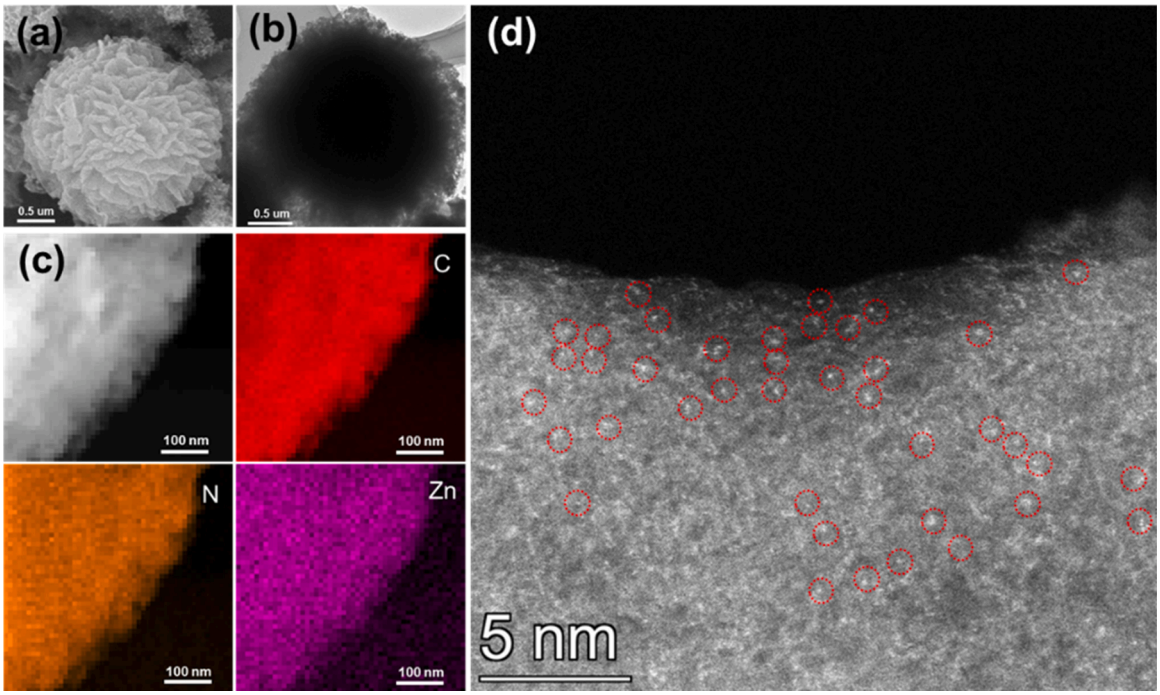

Fig. 2. Morphology of Zn-TpPa. SEM (**a**) and TEM (**b**) figures of Zn-TpPa. **c**. element mapping images of Zn-TpPa. **d**. AC-HAADF-STEM images of Zn-TpPa (Dotted red circles highlight isolated Zn atoms).

portion pores of TpPa-1. We also characterized the CO_2 adsorption capacity of TpPa-1 and Zn-TpPa (Fig. S2). The CO_2 uptake of TpPa-1 was measured as 29 cm^3/g at 273 K up to 1 bar. The CO_2 uptake of Zn-TpPa was as high as 24 cm^3/g, which was comparable (MOF-808, 30 cm^3/g) [71] or higher than (PMO-CPF, 19 cm^3/g) [72] the values of many reported porous materials [73–75]. The results indicated that Zn-TpPa have good adsorption of CO_2 contributing to the high catalytic performance.

We also prepared M-TpPa (M = Pd, Pt, Ni) by replacing Zn^{2+} by Pd^{2+}, Pt^{2+} and Ni^{2+}, respectively. The ICP-OES, XPS and other experiments for Pd-TpPa, Pt-TpPa and Ni-TpPa are shown in supporting information and prove these ions were successfully coordinated to TpPa-1 with no structural collapse of COFs.

3.2. Catalytic activity

The successful immobilization of single Zn atoms into the channels of COFs, which maintains their excellent stability, crystallinity, and porosity, stimulates us to evaluate their performance in heterogeneous catalysis. We utilized N-methylaniline (denoted as **1a**) as a substrate and $PhSiH_3$ as a reductant to perform the CO_2 reductive functionalization as a benchmark reaction.

We first screen the reaction conditions on N-formylation of N-methylaniline (**1a**, Fig. S7b) with CO_2 and $PhSiH_3$ to produce N-methylformanilide (denoted as **1b**, Fig. S7d) and examined the influence of different solvents and potential catalysts based on TpPa-1 at 30 °C and CO_2 (1 atm, balloon) in the presence of 2.0 equiv. of $PhSiH_3$ relative to the amine (Table 1).

Initially, we screened different catalysts such as Pd-TpPa, Pt-TpPa, Ni-TpPa and Zn-TpPa in DMF. Catalyzed by Zn-TpPa, N-methylformanilide was acquired with 99.9 % yield and 99.0 % selectivity in 18 h (**Entry 1**). Using Ni-TpPa as catalyst, achieved 75.1 % conversion to N-methylformanilide with 71.8 % yield and 95.7 % selectivity in 24 h (**Entry 4**). Pd-TpPa and Pt-TpPa were less efficient with 38.4 % and 8.7

Table 1
Reaction condition screening for the N-formylation of N-methylaniline with 1 bar CO_2 pressure and $PhSiH_3$.

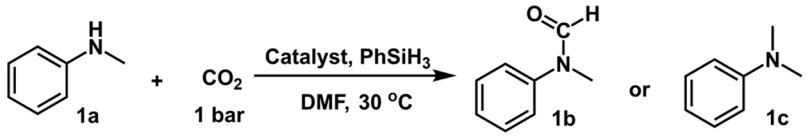

Entry	Catalyst	$PhSiH_3$ (equiv.)	Solvent	Time (h)	C_{1a} (%)	Y_{1b} (%)	Y_{1c} (%)	S_{1b} (%)
1	Zn-TpPa	2	DMF	18	99.9	99.0	0	99.0
2	Pd-TpPa	2	DMF	24	41.2	38.4	2.8	93.3
3	Pt-TpPa	2	DMF	24	14.9	8.7	6.2	58.2
4	Ni-TpPa	2	DMF	24	75.1	71.8	3.3	95.7
5	$ZnCl_2$	2	DMF	24	83.5	82.0	1.5	98.1
6	TpPa-1	2	DMF	24	53.7	52.9	0.8	98.5
7	Zn-TpPa	2	CH_3CN	24	0.7	0	0.7	0
8	Zn-TpPa	2	CH_3OH	24	1.0	0	1.0	0
9	Zn-TpPa	0	DMF	24	0	0	0	0
10	Zn-TpPa	2	DMF	24	0	0	0	0
11	Zn-TpPa	1	DMF	18	28.1	27.1	1.0	96.4
12	Zn-TpPa	3	DMF	18	99.7	86.9	12.8	87.2

% yield in 24 h, respectively (**Entry 2** and **3**). Evidently, Zn-TpPa showed the best catalytic ability among the M-TpPa in this work. Thus, we chose Zn-TpPa as catalyst in subsequent experiments. We also examined the activity of $ZnCl_2$ (**Entry 5**, 82.0 % yield) and TpPa-1 (**Entry 6**, 52.9 % yield), they both showed less efficient than Zn-TpPa, which indicated the excellent catalytic ability of Zn-TpPa originated from the synergistic effect of Zn^{2+} and TpPa-1.

Subsequently, we investigated the influence of several solvents catalyzed by Zn-TpPa. Compared with using DMF as solvent which had 99.9 % yield of N-methylformanilide (denoted as **1b**, Fig. S7c, **Entry 4**) in 18 h, in CH_3CN and CH_3OH, N-methylaniline was only converted to trace amount of N, N-dimethylaniline (denoted as **1c**, **Entry 7** and **8**,) with 0.7 % yield and 1.0 % yield, respectively in 24 h. To prove the C1 source of N-methylformanilide is CO_2 rather than DMF, we performed two control experiments. In **Entry 9**, we used DMF as solvent at 1 bar N_2 pressure, without the addition of $PhSiH_3$ compared to **Entry 4**, we found no existence of **1b**. In **Entry 10**, we used DMF as solvent at 1 bar N_2 pressure with the addition of 2 equiv. $PhSiH_3$, we neither found the existence of **1b**. From the results, we inferred that CO_2 is the C1 source for the N-formylation of N-methylaniline. We also varied different reaction temperatures to optimize the reaction conditions (Fig. 3a and Table S2). By varying the temperatures in the range in between 0–60 °C, the reaction reached the highest yield 99.9 % at 30 °C in 18 h. We also screened the amount of $PhSiH_3$ to get the N-methylated product. One equivalent of $PhSiH_3$ (**Entry 11**) relative to N-methylaniline (**1a**) is insufficient to get N-methylformanilide (**1b**) with high yield (27.1 %). Three equiv. of $PhSiH_3$ (**Entry 12**) is less efficient with relative low selectivity (87.2 %) of **1b** than two equiv. (99.9 %, **Entry 1**). From all the results above, we concluded the reaction condition using DMF as solvent, two equiv. of $PhSiH_3$ as reducing agent, catalyzed by Zn-TpPa and at 30 °C was the optimal condition. The catalytic recyclability of our catalyst was also checked. Fig. 3c proved the catalyst was very efficient (all more than 95 % yield and 95 % selectivity) after five cycles.

Kinetic experiments were carried out to further investigate the catalyst performance (Fig. 3b and Table S2). In 3 h, the reaction reached a yield of 77.2 % and a selectivity of 98.3 %. The Turnover frequency (TOF) 17,155 h^{-1} is the highest among all reported Zn-based catalysts using hydrosilanes as reductants (Table S1), verifying the superiority of single atom catalysts. Importantly, Zn-TpPa showed the highest TOF among the reported catalysts which catalyzed N-formylation of N-methylaniline with CO_2 and hydrosilanes with good recyclability (Fig. 3d) [6–8,10,11,13–16,21,24–30,32–40,76–89].Subsequently, after 6 h, the reaction reached 92.3 % yield with the still highest TOF 10,255 h^{-1} among the reported benchmarks (Fig. 3d).

Under the optimized reaction conditions, investigation of the substrate scope was performed (Table 2). We found aromatic amines, heterocyclic amines and aliphatic amines were readily N-formylated to the

Table 2
N-formylation of various amines with CO_2 and $PhSiH_3$ catalyzed by Zn-TpPa.

	Substrate	Product	C_a (%)	Y_b (%)
S1			99.9	99.9
S2		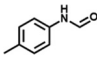	79.8	79.8
S3			99.9	98.7
S4			99.9	99.2
S5			99.9	98.0
S6			99.9	99.9
S7			99.9	99.9
S8			99.9	99.9
S9			99.9	99.9

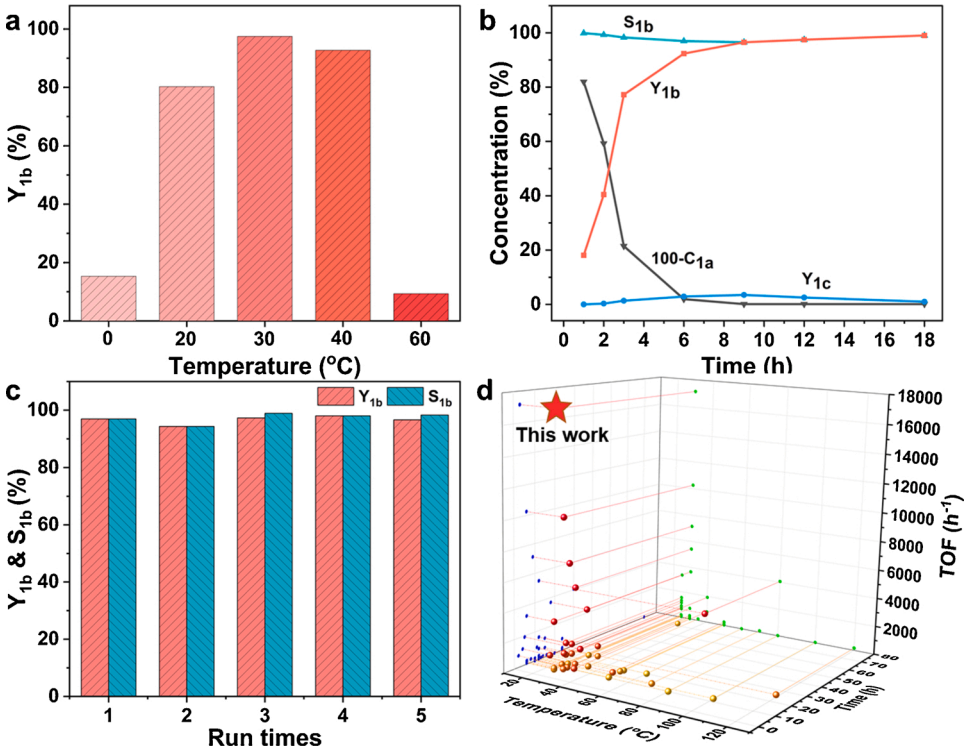

Fig. 3. Catalyst performance. **a**. Temperature screening for N-formylation of N-methylaniline in 12 h (60 °C in 48 h). **b**. Kinetic curve of the reaction at 30 °C. **c**. Recyclability test of the catalyst in 12 h. d. TOF comparison with benchmark literatures.

corresponding formamides in excellent yields with Zn-TpPa. Firstly, primary amines such as aniline and p-toluidine were quantitatively converted to the desired formamides (**S1** and **S2**), respectively, with excellent selectivity and yield. Electron-donating aromatic amines such as Me and OMe derivatives and electron-withdrawing aromatic 4-bromo-N-methylaniline afforded the desired compounds (**S1**-**S5**) with 79.8–99.9 % yields respectively. Fortunately, this method was also successful in the N-formylation of aliphatic diethylamine with 99.9 % yield (**S6**). Moreover, heterocyclic amines such as N-methylcyclohexylamine (**S7**), pyrrolidine (**S8**) and morpholine (**S9**) all showed good to excellent reactivity (99.9 % yield and 99.9 % selectivity). The results indicated Zn-TpPa had excellent availability for N-formylation of both primary amines and secondary amines, as well as aromatic amines, heterocyclic amines and aliphatic amines.

Zn-TpPa showed excellent catalytic activity for N-formylation, which could be explained by the next mechanism. Zn^{2+} provided the active site, as well as amine functionalized TpPa-1 absorbed more CO_2, which increased the local concentration of carbon dioxide. [1,63,90,91] Firstly, Zn-TpPa has atomically dispersed Zinc, which regarded as active center for N-formylation [10,27]. Secondly, it showed excellent surface area, and could adsorb and accumulate CO_2 for the reaction system. [63] The ordered open channels and high CO_2 uptake capacity of the Zn-TpPa allow formylation reactions to be conducted under mild conditions. The highest TOF of 17,155 h^{-1} has been normalized to single Zn sites, proving the highest reactivity. In the N-formylation reaction of amine with $PhSiH_3$ and CO_2 over Zn-TpPa, the zinc center activates the Si–H bond of $PhSiH_3$. This affords the highly active zinc–hydrogen (Zn–H) species and permits a mechanism that involves the transition-metal-promoted hydride transfer from $PhSiH_3$ to CO_2, based on an intermediate silyl formate. [80] In other words, Zn-TpPa could active $PhSiH_3$ to react with CO_2 yielding formoxysilane, [33] and simultaneously activated the amine to obtain the desired product (Fig. S5).

4. Conclusion

In conclusion, Zn single atom catalyst on COF with high loading were facially prepared. Zn-TpPa showed excellent catalyst activity, selectivity and recyclability for N-formation under mild condition with CO_2 and phenysilane. It showed the highest TOF normalized to single Zn sites as 17,155 h^{-1} among all reported Zn-based catalysts. Importantly, Zn-TpPa showed the highest TOF among all reported catalysts which promoted N-formylation of N-methylaniline with CO_2 and hydrosilanes with good recyclability. Besides, Zn-TpPa could catalyze N-formylation of many other amines with excellent yields. This facile method provides the possibility to prepare more single atom catalysts in large-scale. The efficient catalyst is beneficial for CO_2 transformation and environmental protection.

CRediT authorship contribution statement

Qiang Cao: Investigation, Conceptualization, Writing - original draft. **Long-Long Zhang:** Data curation. **Chang Zhou:** Resources. **Jing-Hui He:** Supervision, Writing - review & editing, Funding acquisition. **Antonio Marcomini:** Writing - review & editing. **Jian-Mei Lu:** Resources, Writing - review & editing, Supervision, Funding acquisition.

Declaration of Competing Interest

The authors report no declarations of interest.

Acknowledgements

We gratefully acknowledge the financial support provided by National Natural Science Foundation of China (21978185, 21938006, 21776190), the National Key R&D Program of China (2020YFC1818401, 2017YFC0210906), Basic Research Project of Leading Technology in Jiangsu Province (BK20202012), Suzhou Science and Technology Bureau Project (SYG201935) and the project supported by the Priority Academic Program Development of Jiangsu Higher Education Institutions (PAPD).

Appendix A. Supplementary data

Supplementary material related to this article can be found, in the online version, at doi:https://doi.org/10.1016/j.apcatb.2021.120238.

References

[1] T.M. McDonald, W.R. Lee, J.A. Mason, B.M. Wiers, C.S. Hong, J.R. Long, Capture of carbon dioxide from air and flue gas in the alkylamine-appended metal-organic framework mmen-Mg2(dobpdc), J. Am. Chem. Soc. 134 (2012) 7056–7065.
[2] Q. He, J.H. Lee, D. Liu, Y. Liu, Z. Lin, Z. Xie, S. Hwang, S. Kattel, L. Song, J.G. Chen, Accelerating CO2 electroreduction to CO over Pd single-atom catalyst, Adv. Funct. Mater. 30 (2020), 2000407.
[3] R.P. Ye, Q.H. Li, W.B. Gong, T.T. Wang, J.J. Razink, L. Lin, Y.Y. Qin, Z.F. Zhou, H. Adidharma, J.K. Tang, A.G. Russell, M.H. Fan, Y.G. Yao, High-performance of nanostructured Ni/CeO2 catalyst on CO2 methanation, Appl. Catal. B 268 (2020), 118474.
[4] B. Yang, H. Xu, Y.B. Liu, F. Li, X.S. Song, Z.W. Wang, W. Sand, Role of GAC-MnO2 catalyst for triggering the extracellular electron transfer and boosting CH4 production in syntrophic methanogenesis, Chem. Eng. J. 383 (2020), 123211.
[5] H. Kumagai, T. Nishikawa, H. Koizumi, T. Yatsu, G. Sahara, Y. Yamazaki, Y. Tamaki, O. Ishitani, Electrocatalytic reduction of low concentration CO2, Chem. Sci. 10 (2019) 1597–1606.
[6] X.F. Liu, X.Y. Li, C. Qiao, H.C. Fu, L.N. He, Betaine catalysis for hierarchical reduction of CO2 with amines and hydrosilane to form formamides, aminals, and methylamines, Angew. Chem. Int. Ed. Engl. 56 (2017) 7425–7429.
[7] J. Song, B. Zhou, H. Liu, C. Xie, Q. Meng, Z. Zhang, B. Han, Biomass-derived γ-valerolactone as an efficient solvent and catalyst for the transformation of CO2 to formamides, Green Chem. 18 (2016) 3956–3961.
[8] M. Hulla, F.D. Bobbink, S. Das, P.J. Dyson, Carbon dioxide based N-formylation of amines catalyzed by fluoride and hydroxide anions, ChemCatChem 8 (2016) 3338–3342.
[9] M. Aresta, A. Dibenedetto, A. Angelini, Catalysis for the valorization of exhaust carbon: from CO2 to chemicals, materials, and fuels. Technological use of CO2, Chem. Rev. 114 (2014) 1709–1742.
[10] R. Luo, X. Lin, Y. Chen, W. Zhang, X. Zhou, H. Ji, Cooperative catalytic activation of Si-H bonds: CO2 -Based synthesis of formamides from amines and hydrosilanes under mild conditions, ChemSusChem 10 (2017) 1224–1232.
[11] M. Hulla, D. Ortiz, S. Katsyuba, D. Vasilyev, P.J. Dyson, Delineation of the critical parameters of salt catalysts in the N-Formylation of amines with CO2, Chem. - Eur. J. 25 (2019) 11074–11079.
[12] M. Hulla, S. Nussbaum, A.R. Bonnin, P.J. Dyson, The dilemma between acid and base catalysis in the synthesis of benzimidazole from o-phenylenediamine and carbon dioxide, Chem. Commun. 55 (2019) 13089–13092.
[13] Y. Chen, R. Luo, J. Bao, Q. Xu, J. Jiang, X. Zhou, H. Ji, Function-oriented ionic polymers having high-density active sites for sustainable carbon dioxide conversion, J. Mater. Chem. A 6 (2018) 9172–9182.
[14] M. Hulla, G. Laurenczy, P.J. Dyson, Mechanistic study of the N-Formylation of amines with carbon dioxide and hydrosilanes, ACS Catal. 8 (2018) 10619–10630.
[15] Q. Shen, X. Chen, Y. Tan, J. Chen, L. Chen, S. Tan, Metal-free N-formylation of amines with CO2 and hydrosilane by nitrogen-doped graphene nanosheets, ACS Appl. Mater. Interfaces 11 (2019) 38838–38848.
[16] A. Gopakumar, L. Lombardo, Z.F. Fei, S. Shyshkanov, D. Vasilyev, A. Chidambaram, K. Stylianou, A. Zuttel, P.J. Dyson, A polymeric ionic liquid catalyst for the N-formylation and N-methylation of amines using CO2/PhSiH3, J. CO2 Util. 41 (2020), 101240.
[17] P. Bhanja, A. Modak, A. Bhaumik, Supported porous nanomaterials as efficient heterogeneous catalysts for CO2 fixation reactions, Chem. – Eur. J. 24 (2018) 7278–7297.
[18] A. Modak, P. Bhanja, S. Dutta, B. Chowdhury, A. Bhaumik, Catalytic reduction of CO2 into fuels and fine chemicals, Green Chem. 22 (2020) 4002–4033.
[19] A. Modak, P. Bhanja, A. Bhaumik, Microporous nanotubes and nanospheres with iron-catechol sites: efficient lewis acid catalyst and support for Ag nanoparticles in CO2 fixation reaction, Chem - Eur J 24 (2018) 14189–14197.
[20] P. Bhanja, A. Modak, A. Bhaumik, Porous organic polymers for CO2 storage and conversion reactions, ChemCatChem 11 (2018) 244–257.
[21] R.A. Molla, P. Bhanja, K. Ghosh, S.S. Islam, A. Bhaumik, S.M. Islam, Pd nanoparticles decorated on hypercrosslinked microporous polymer: a highly efficient catalyst for the formylation of amines through carbon dioxide fixation, ChemCatChem 9 (2017) 1939–1946.
[22] S.K. Das, S. Chatterjee, S. Bhunia, A. Mondal, P. Mitra, V. Kumari, A. Pradhan, A. Bhaumik, A new strongly paramagnetic cerium-containing microporous MOF for CO2 fixation under ambient conditions, Dalton Trans. 46 (2017) 13783–13792.
[23] A.H. Chowdhury, P. Bhanja, N. Salam, A. Bhaumik, S.M. Islam, Magnesium oxide as an efficient catalyst for CO 2 fixation and N-formylation reactions under ambient conditions, Mol. Catal. 450 (2018) 46–54.

[24] S.Q. Zhang, Q.Q. Mei, H.Y. Liu, H.Z. Liu, Z.P. Zhang, B.X. Han, Copper-catalyzed N-formylation of amines with CO2 under ambient conditions, RSC Adv. 6 (2016) 32370–32373.
[25] K. Motokura, N. Takahashi, D. Kashiwame, S. Yamaguchi, A. Miyaji, T. Baba, Copper-diphosphine complex catalysts for N-formylation of amines under 1 atm of carbon dioxide with polymethylhydrosiloxane, Catal. Sci. Technol. 3 (2013) 2392–2396.
[26] R.C. Luo, X.W. Lin, J. Lu, X.T. Zhou, H.B. Ji, Zinc phthalocyanine as an efficient catalyst for halogen-free synthesis of formamides from amines via carbon dioxide hydrosilylation under mild conditions, Chin. J. Catal. 38 (2017) 1382–1389.
[27] W.Y. Zhang, R.C. Luo, Q.H. Xu, Y.J. Chen, X.W. Lin, X.T. Zhou, H.B. Ji, Transformation of carbon dioxide into valuable chemicals over bifunctional metallosalen catalysts bearing quaternary phosphonium salts, Chin. J. Catal. 38 (2017) 736–744.
[28] Z. Huang, X. Jiang, S. Zhou, P. Yang, C.X. Du, Y. Li, Mn-catalyzed selective double and mono-N-formylation and N-methylation of amines by using CO2, ChemSusChem 12 (2019) 3054–3059.
[29] Q. Zhang, X.T. Lin, N. Fukaya, T. Fujitani, K. Sato, J.C. Choi, Selective N-formylation/N-methylation of amines and N-formylation of amides and carbamates with carbon dioxide and hydrosilanes: promotion of the basic counter anions of the zinc catalyst, Green Chem. 22 (2020) 8414–8422.
[30] K. Takaishi, B.D. Nath, Y. Yamada, H. Kosugi, T. Ema, Unexpected macrocyclic multinuclear zinc and nickel complexes that function as multitasking catalysts for CO2 fixations, Angew. Chem. Int. Ed. Engl. 58 (2019) 9984–9988.
[31] S. Kozuch, J.M.L. Martin, "Turning Over" definitions in catalytic cycles, ACS Catal. 2 (2012) 2787–2794.
[32] S. Ghosh, A. Ghosh, S. Biswas, M. Sengupta, D. Roy, S.M. Islam, Palladium grafted functionalized nanomaterial: an efficient catalyst for the CO2 fixation of amines and production of organic carbamates, Chemistryselect 4 (2019) 3961–3972.
[33] B. Dong, L. Wang, S. Zhao, R. Ge, X. Song, Y. Wang, Y. Gao, Immobilization of ionic liquids to covalent organic frameworks for catalyzing the formylation of amines with CO2 and phenylsilane, Chem. Commun. 52 (2016) 7082–7085.
[34] X.L. Jiang, Z.J. Huang, M. Makha, C.X. Du, D.M. Zhao, F. Wang, Y.H. Li, Tetracoordinate borates as catalysts for reductive formylation of amines with carbon dioxide, Green Chem. 22 (2020) 5317–5324.
[35] G. Li, J. Chen, D.Y. Zhu, Y. Chen, J.B. Xia, DBU-catalyzed selective N-methylation and N-formylation of amines with CO2 and polymethylhydrosiloxane, Adv. Synth. Catal. 360 (2018) 2364–2369.
[36] R. Khatun, S. Biswas, S. Islam, I.H. Biswas, S. Riyajuddin, K. Ghosh, S.M. Islam, Modified graphene oxide based zinc composite: an efficient catalyst for N-formylation and carbamate formation reactions through CO2 fixation, ChemCatChem 11 (2019) 1303–1312.
[37] C. Du, Y. Chen, Zinc powder catalysed formylation and urealation of amines using CO2 as a C1 building block †, Chin. J. Chem. 38 (2020) 1057–1064.
[38] M.Y. Wang, N. Wang, X.F. Liu, C. Qiao, L.N. He, Tungstate catalysis: pressure-switched 2-and 6-electron reductive functionalization of CO2 with amines and phenylsilane, Green Chem. 20 (2018) 1564–1570.
[39] P.B. Wang, Q. He, H. Zhang, Q.D. Sun, Y.J. Cheng, T. Gan, X.H. He, H.B. Ji, N-formylation of amines using phenylsilane and CO2 over ZnO catalyst under mild condition, Catal. Commun. 149 (2021), 106195.
[40] A. Gopakumar, I. Akçok, L. Lombardo, F. Le Formal, A. Magrez, K. Sivula, P. J. Dyson, Iron-rich natural mineral gibeon meteorite catalyzed N-formylation of amines using CO2 as the C1 source, ChemistrySelect 3 (2018) 10271–10276.
[41] S.K. Kaiser, Z. Chen, D. Faust Akl, S. Mitchell, J. Perez-Ramirez, Single-atom catalysts across the periodic table, Chem. Rev. 120 (2020) 11703–11809.
[42] L. Zhang, M. Zhou, A. Wang, T. Zhang, Selective hydrogenation over supported metal catalysts: from nanoparticles to single atoms, Chem. Rev. 120 (2020) 683–733.
[43] Y.S. Wei, M. Zhang, R. Zou, Q. Xu, Metal-organic framework-based catalysts with single metal sites, Chem. Rev. 120 (2020) 12089–12174.
[44] S. Ji, Y. Chen, X. Wang, Z. Zhang, D. Wang, Y. Li, Chemical synthesis of single atomic site catalysts, Chem. Rev. 120 (2020) 11900–11955.
[45] S. Bai, F. Liu, B. Huang, F. Li, H. Lin, T. Wu, M. Sun, J. Wu, Q. Shao, Y. Xu, X. Huang, High-efficiency direct methane conversion to oxygenates on a cerium dioxide nanowires supported rhodium single-atom catalyst, Nat. Commun. 11 (2020) 954.
[46] W. Zang, Z. Kou, S.J. Pennycook, J. Wang, Heterogeneous single atom electrocatalysis, where "Singles" are "Married", Adv. Energy Mater. 10 (2020), 1903181.
[47] N. Cheng, S. Stambula, D. Wang, M.N. Banis, J. Liu, A. Riese, B. Xiao, R. Li, T. K. Sham, L.M. Liu, G.A. Botton, X. Sun, Platinum single-atom and cluster catalysis of the hydrogen evolution reaction, Nat. Commun. 7 (2016), 13638.
[48] B. Qiao, A. Wang, X. Yang, L.F. Allard, Z. Jiang, Y. Cui, J. Liu, J. Li, T. Zhang, Single-atom catalysis of CO oxidation using Pt1/FeOx, Nat. Chem. 3 (2011) 634–641.
[49] C. Zhao, X. Dai, T. Yao, W. Chen, X. Wang, J. Wang, J. Yang, S. Wei, Y. Wu, Y. Li, Ionic exchange of metal-organic frameworks to access single nickel sites for efficient electroreduction of CO2, J. Am. Chem. Soc. 139 (2017) 8078–8081.
[50] L. Zhang, L. Han, H. Liu, X. Liu, J. Luo, Potential-cycling synthesis of single platinum atoms for efficient hydrogen evolution in neutral media, Angew. Chem. Int. Ed. Engl. 56 (2017) 13694–13698.
[51] F. Li, G.F. Han, H.J. Noh, S.J. Kim, Y.L. Lu, H.Y. Jeong, Z.P. Fu, J.B. Baek, Boosting oxygen reduction catalysis with abundant copper single atom active sites, Energy Environ. Sci. 11 (2018) 2263–2269.
[52] P. Liu, Y. Zhao, R. Qin, S. Mo, G. Chen, L. Gu, D.M. Chevrier, P. Zhang, Q. Guo, D. Zang, B. Wu, G. Fu, N. Zheng, Photochemical route for synthesizing atomically dispersed palladium catalysts, Science 352 (2016) 797–801.
[53] Y. Shi, S. Liu, Z. Zhang, Y. Liu, M. Pang, Template-free synthesis and metalation of hierarchical covalent organic framework spheres for photothermal therapy, Chem. Commun. 55 (2019) 14315–14318.
[54] P. Sun, J. Hai, S. Sun, S. Lu, S. Liu, H. Liu, F. Chen, B. Wang, Aqueous stable Pd nanoparticles/covalent organic framework nanocomposite: an efficient nanoenzyme for colorimetric detection and multicolor imaging of cancer cells, Nanoscale 12 (2020) 825–831.
[55] D. Mullangi, D. Chakraborty, A. Pradeep, V. Koshti, C.P. Vinod, S. Panja, S. Nair, R. Vaidhyanathan, Highly stable COF-Supported Co/Co(OH)2 nanoparticles heterogeneous catalyst for reduction of Nitrile/Nitro compounds under mild conditions, Small 14 (2018), 1801233.
[56] A.P. Cote, A.I. Benin, N.W. Ockwig, M. O'Keeffe, A.J. Matzger, O.M. Yaghi, Porous, crystalline, covalent organic frameworks, Science 310 (2005) 1166–1170.
[57] H. Zhong, R. Sa, H. Lv, S. Yang, D. Yuan, X. Wang, R. Wang, Covalent organic framework hosting metalloporphyrin-based carbon dots for visible-light-driven selective CO2 reduction, Adv. Funct. Mater. 30 (2020).
[58] S.M.J. Rogge, A. Bavykina, J. Hajek, H. Garcia, A.I. Olivos-Suarez, A. Sepulveda-Escribano, A. Vimont, G. Clet, P. Bazin, F. Kapteijn, M. Daturi, E.V. Ramos-Fernandez, I.X.F.X. Llabres, V. Van Speybroeck, J. Gascon, Metal-organic and covalent organic frameworks as single-site catalysts, Chem. Soc. Rev. 46 (2017) 3134–3184.
[59] B. Sun, X. Li, T. Feng, S. Cai, T. Chen, C. Zhu, J. Zhang, D. Wang, Y. Liu, Resistive switching memory performance of two-dimensional polyimide covalent organic framework films, ACS Appl. Mater. Interfaces 12 (2020) 51837–51845.
[60] S. Xu, Q. Zhang, Recent progress in covalent organic frameworks as light-emitting materials, Mater. Today Energy (2021), 100635.
[61] R. Qin, K. Liu, Q. Wu, N. Zheng, Surface coordination chemistry of atomically dispersed metal catalysts, Chem. Rev. 120 (2020) 11810–11899.
[62] J. H. He, J. M. Lu, Patent. (2021) 202110127803.3.
[63] S. Kandambeth, A. Mallick, B. Lukose, M.V. Mane, T. Heine, R. Banerjee, Construction of crystalline 2D covalent organic frameworks with remarkable chemical (acid/base) stability via a combined reversible and irreversible route, J. Am. Chem. Soc. 134 (2012) 19524–19527.
[64] D. Zhu, R. Verduzco, Ultralow surface tension solvents enable facile COF activation with reduced pore collapse, ACS Appl. Mater. Interfaces 12 (2020) 33121–33127.
[65] J. Wang, L. Zhao, B. Yan, Indicator displacement assay inside dye-functionalized covalent organic frameworks for ultrasensitive monitoring of sialic acid, an ovarian cancer biomarker, ACS Appl. Mater. Interfaces 12 (2020) 12990–12997.
[66] X. Yin, J.Z. Low, K.J. Fallon, D.W. Paley, L.M. Campos, The butterfly effect in bisfluorenylidene-based dihydroacenes: aggregation induced emission and spin switching, Chem. Sci. 10 (2019) 10733–10739.
[67] M.A. Khayum, M. Ghosh, V. Vijayakumar, A. Halder, M. Nurhuda, S. Kumar, M. Addicoat, S. Kurungot, R. Banerjee, Zinc ion interactions in a two-dimensional covalent organic framework based aqueous zinc ion battery, Chem. Sci. 10 (2019) 8889–8894.
[68] P.Á. Szilágyi, D.M. Rogers, I. Zaiser, E. Callini, S. Turner, A. Borgschulte, A. Züttel, H. Geerlings, M. Hirscher, B. Dam, Functionalised metal–organic frameworks: a novel approach to stabilising single metal atoms, J. Mater. Chem. A 5 (2017) 15559–15566.
[69] J. Wang, H. Li, S. Liu, Y. Hu, J. Zhang, M. Xia, Y. Hou, J. Tse, J. Zhang, Y. Zhao, Turning on Zn 4s electrons in a N2 -Zn-B2 configuration to stimulate remarkable ORR performance, Angew. Chem. Int. Ed. Engl. 60 (2021) 181–185.
[70] J. Li, S. Chen, N. Yang, M. Deng, S. Ibraheem, J. Deng, J. Li, L. Li, Z. Wei, Ultrahigh-loading zinc single-atom catalyst for highly efficient oxygen reduction in both acidic and alkaline media, Angew. Chem. Int. Ed. Engl. 58 (2019) 7035–7039.
[71] J.M. Park, D.K. Yoo, S.H. Jhung, Selective CO2 adsorption over functionalized Zr-based metal organic framework under atmospheric or lower pressure: contribution of functional groups to adsorption, Chem. Eng. J. 402 (2020), 126254.
[72] X. Cheng, P. Zhao, M. Zhang, S. Wang, M. Liu, F. Liu, Fabrication of robust and bifunctional cyclotriphosphazene-based periodic mesoporous organosilicas for efficient CO2 adsorption and catalytic conversion, Chem. Eng. J. 418 (2021), 129360.
[73] Y. Meng, Y. Luo, J.L. Shi, H. Ding, X. Lang, W. Chen, A. Zheng, J. Sun, C. Wang, 2D and 3D porphyrinic covalent organic frameworks: the influence of dimensionality on functionality, Angew. Chem. Int. Ed. Engl. 59 (2020) 3624–3629.
[74] X. Liu, G.J.H. Lim, Y. Wang, L. Zhang, D. Mullangi, Y. Wu, D. Zhao, J. Ding, A. K. Cheetham, J. Wang, Binder-free 3D printing of covalent organic framework (COF) monoliths for CO2 adsorption, Chem. Eng. J. 403 (2021), 126333.
[75] M. Liu, X. Lu, L. Shi, F. Wang, J. Sun, Periodic mesoporous organosilica with a basic urea-derived framework for enhanced carbon dioxide capture and conversion under mild conditions, ChemSusChem 10 (2017) 1110–1119.
[76] C. Fang, C.L. Lu, M.H. Liu, Y.L. Zhu, Y. Fu, B.L. Lin, Selective formylation and methylation of amines using carbon dioxide and hydrosilane catalyzed by alkali-metal carbonates, ACS Catal. 6 (2016) 7876–7881.
[77] X.D. Li, S.M. Xia, K.H. Chen, X.F. Liu, H.R. Li, L.N. He, Copper catalysis: ligand-controlled selective N-methylation or N-formylation of amines with CO2 and phenylsilane, Green Chem. 20 (2018) 4853–4858.
[78] T. Murata, M. Hiyoshi, M. Ratanasak, J.Y. Hasegawa, T. Ema, Synthesis of silyl formates, formamides, and aldehydes via solvent-free organocatalytic hydrosilylation of CO2, Chem. Commun. 56 (2020) 5783–5786.
[79] W.F. Zhao, X.P. Chi, H. Li, J. He, J.X. Long, Y.F. Xu, S. Yang, Eco-friendly acetylcholine-carboxylate bio-ionic liquids for controllable N-methylation and N-

formylation using ambient CO2 at low temperatures, Green Chem. 21 (2019) 567–577.
[80] X.F. Liu, R. Ma, C. Qiao, H. Cao, L.N. He, Fluoride-catalyzed methylation of amines by reductive functionalization of CO2 with hydrosilanes, Chem. - Eur. J. 22 (2016) 16489–16493.
[81] Y. Hu, J.L. Song, C. Xie, H.R. Wu, Z.P. Wang, T. Jiang, L. Wu, Y. Wang, B.X. Han, Renewable and biocompatible lecithin as an efficient organocatalyst for reductive conversion of CO2 with amines to formamides and methylamines, ACS Sustain. Chem. Eng. 6 (2018) 11228–11234.
[82] W.D. Li, D.Y. Zhu, G. Li, J. Chen, J.B. Xia, Iron-catalyzed selective N-methylation and N-formylation of amines with CO2, Adv. Synth. Catal. 361 (2019) 5098–5104.
[83] Z.J. Mu, X. Ding, Z.Y. Chen, B.H. Han, Zwitterionic covalent organic frameworks as catalysts for hierarchical reduction of CO2 with amine and hydrosilane, ACS Appl. Mater. Interfaces 10 (2018) 41350–41358.
[84] R.H. Lam, C.M.A. McQueen, I. Pernik, R.T. McBurney, A.F. Hill, B.A. Messerle, Selective formylation or methylation of amines using carbon dioxide catalysed by a rhodium perimidine-based NHC complex, Green Chem. 21 (2019) 538–549.
[85] X.Y. Li, H.C. Fu, X.F. Liu, S.H. Yang, K.H. Chen, L.N. He, Design of Lewis base functionalized ionic liquids for the N-formylation of amines with CO2 and hydrosilane: the cation effects, Catal. Today 356 (2020) 563–569.
[86] H. Lv, W. Wang, F. Li, Porous organic polymers with built-in N-heterocyclic carbenes: selective and efficient heterogeneous catalyst for the reductive N-formylation of amines with CO2, Chem. - Eur. J. 24 (2018) 16588–16594.
[87] X.F. Liu, C. Qiao, X.Y. Li, L.N. He, Carboxylate-promoted reductive functionalization of CO2 with amines and hydrosilanes under mild conditions, Green Chem. 19 (2017) 1726–1731.
[88] H. Lv, Q. Xing, C. Yue, Z. Lei, F. Li, Solvent-promoted catalyst-free N-formylation of amines using carbon dioxide under ambient conditions, Chem. Commun. 52 (2016) 6545–6548.
[89] X.F. Liu, C. Qiao, X.Y. Li, L.N. He, DMF-promoted reductive functionalization of CO2 with secondary amines and phenylsilane to methylamines, Pure Appl. Chem. 90 (2018) 1099–1107.
[90] W.G. Lu, J.P. Sculley, D.Q. Yuan, R. Krishna, H.C. Zhou, Carbon dioxide capture from air using amine-grafted porous polymer networks, J. Phys. Chem. C 117 (2013) 4057–4061.
[91] P.Q. Liao, X.W. Chen, S.Y. Liu, X.Y. Li, Y.T. Xu, M. Tang, Z. Rui, H. Ji, J.P. Zhang, X. M. Chen, Putting an ultrahigh concentration of amine groups into a metal-organic framework for CO2 capture at low pressures, Chem. Sci. 7 (2016) 6528–6533.